THE IMPACT OF LEE-SIDE STATIC STABILITY ON THE DISTRIBUTION OF OROGRAPHIC PRECIPITATION

Günther Zängl

Meteorologisches Institut der Universität München, Theresienstraße 37, D-80333 München, Germany
E-mail: *guenther@meteo.physik.uni-muenchen.de*

Abstract: Numerical simulations are presented to examine the effect of the lee-side static stability on the spillover of orographic precipitation. The results show that the presence a cold-air pool in the lee of a mountain ridge greatly increases the precipitation spillover because the cold pool suppresses the lee-side downslope air motion that otherwise leads to a rapid evaporation of the precipitation. The enhancement of the lee-side precipitation reaches up to two orders of magnitude in a nonconvective environment and ranges around one order of magnitude in convective cases. However, the largest absolute spillover is found for a convectively unstable environment because convective cells decay more slowly than stratiform precipitation.

1. INTRODUCTION

In recent years, several idealized numerical studies have been conducted in order to examine dynamical and microphysical aspects of orographic precipitation, both in stable and convective environments. One of the issues that have not been systematically investigated so far is the spillover of orographic precipitation to the lee side of a mountain and its dependence on the lee-side stratification. Intuitively, one expects that a stable layer in the lee of a mountain increases the spillover of precipitation because it reduces the gravity-wave-related subsidence and therefore the evaporation. The main goal of this study is to quantify this effect with the aid of idealized numerical simulations. After describing the setup of the simulations in section 2, the results will be discussed in section 3. The main findings are summarized in section 4.

2. MODEL AND SETUP

The numerical simulations presented in the following have been conducted with the Penn State University – National Center for Atmospheric Research MM5 model, version 3.3 (Grell et al. 1995). The model is used in a configuration with four interactively nested domains, having a horizontal mesh size of 27 km, 9 km, 3 km and 1 km, respectively. In the vertical, 41 full-sigma levels are used, and the vertical resolution ranges between 50 m near the surface and about 700 m near the upper boundary which is located at 100 hPa. The simulations are based on a highly idealized model topography, composed of two elongated mountain ridges in the reference case. The ridges are oriented in meridional direction, and their shape is given by a $\sin^2$-function. They have a maximum height of 2000 m, a base-to-base width of 40 km, and a separation of 200 km. In the first series of sensitivity tests, the mountain ridges are connected by two zonally oriented ridges to form a closed basin. This basin is intended to carry a cold-air pool (see below), providing a layer of high static stability in the lee of the first ridge. In a second series of sensitivity tests, the area enclosed by the four crest lines is filled with matter so as to yield a plateau with a height of 2000 m. This represents a kind of upper limit for the possible effect of a lee-side cold-air pool. Parameterizations are used for cloud microphysics, surface friction and turbulent vertical mixing, but radiation is not taken into account. Further details on the model configuration are provided in Zängl (2005).

The initial and boundary conditions used for the simulations are idealized as well. Here, results are presented for two basic temperature soundings, starting from a sea-level temperature of 290 K and using a tropospheric vertical temperature gradient of $-6.5\,\mathrm{K\,km^{-1}}$ in the convectively unstable case and of $-5.4\,\mathrm{K\,km^{-1}}$ in the (almost) moist neutral case. Above 250 hPa, an isothermal stratosphere is prescribed. The relative humidity is set to 95% between sea level and 500 hPa and then decreases linearly with pressure to 15% at tropopause level. In the simulations with a cold-air filled basin, the cold pool is constructed by reducing the
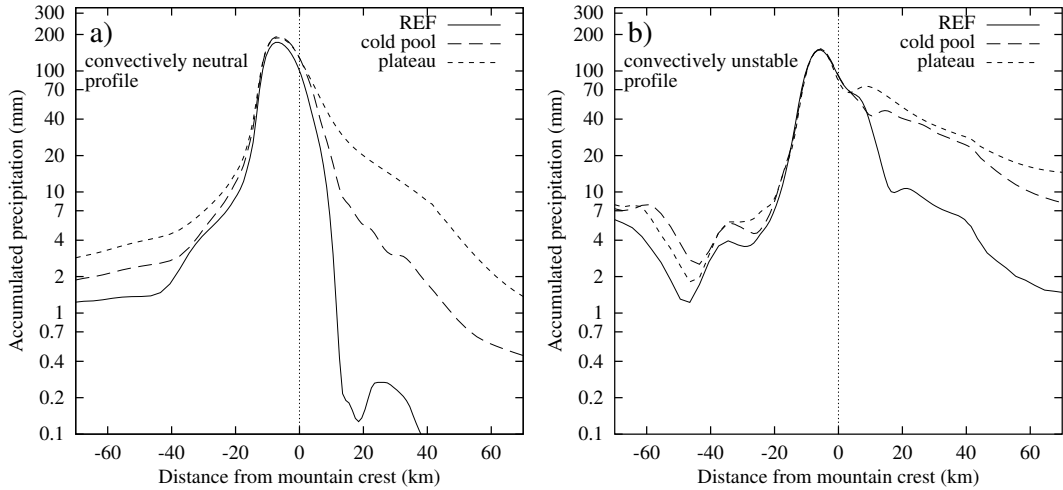
Figure 1: Averaged 24-h accumulated precipitation (mm) for the weak-wind simulations. See text for further explanation.

basic temperature profile below a height of 1500 m by 10 K, topped by a linear transition zone between 1500 m and 2000 m (crest height). The large-scale wind field is a geostrophically balanced cross-ridge flow with positive vertical shear. To avoid spinup problems in the interaction with the cold-air pool, the wind speed at crest level is zero at initial time. During the first six hours of the simulation, the wind and pressure fields imposed at the lateral boundaries are then continuously changed to accelerate the flow. Two different final wind profiles are considered. The first one has a westerly wind of $7.5\,\mathrm{m\,s^{-1}}$ at sea level, increasing linearly with height up to $20\,\mathrm{m\,s^{-1}}$ at tropopause level. The second (stronger) one assumes values of 12.5 and $30\,\mathrm{m\,s^{-1}}$, respectively. Above the tropopause, the wind remains constant with height in each case. The Coriolis parameter relating the wind and pressure fields is set to a constant value of $10^{-4}\,\mathrm{s^{-1}}$ throughout the domain.

3. RESULTS

3.1 Weak-wind simulations

We start our discussion with the simulations based on the "weak" wind profile, ranging from $7.5\,\mathrm{m\,s^{-1}}$ at sea level to $20\,\mathrm{m\,s^{-1}}$ at tropopause level. Fig. 1 depicts the accumulated precipitation after 24 hours of integration. To eliminate the along-ridge fluctuations present in the convective case, the precipitation data are averaged in meridional direction over the central 72 km of the mountain ridge. Note that a logarithmic scale is used to highlight the comparatively small precipitation amounts away from the mountain ridge. For the reference and cold-pool cases, vertical cross-sections of potential temperature and total precipitation mixing ratio (rain + snow + graupel) at $t = 18$h are provided in Fig. 2.

In all cases, the precipitation fields show the familiar picture of a pronounced maximum over the windward slope of the mountain. The peak precipitation accumulation is somewhat higher for the neutral than for the convective case because the former has a higher average temperature and therefore more precipitable water. On the windward side of the mountain, the precipitation field extends into the region of level topography ($x \leq -20$ km) in all simulations. The precipitation amounts far upstream of the mountain are larger for the convective case than for the neutral case because in the former, upstream propagating convective cells occur during the spinup phase of the simulations. Moreover, in the neutral case, the far-upstream precipitation accumulations are influenced by the presence of a lee-side cold pool (or plateau). As discussed in Zängl (2005), this sensitivity is related to a slight change of the gravity-wave pattern aloft. In the cold-pool and plateau cases, the upstream extent of the upper-level lifting is larger than in the reference case, leading to somewhat higher precipitation amounts on the upstream side of the mountain.

Nevertheless, the primary effect of the cold pool on the precipitation field is found in the lee of the mountain, where the presence of a cold pool prevents the formation of downslope flow (Fig. 2) and therefore reduces the evaporative loss of precipitation. The fractional precipitation enhancement in the lee ranges between a factor of 5 in the convective case (Fig. 1b) and almost two orders of magnitude in the nonconvective case (Fig.
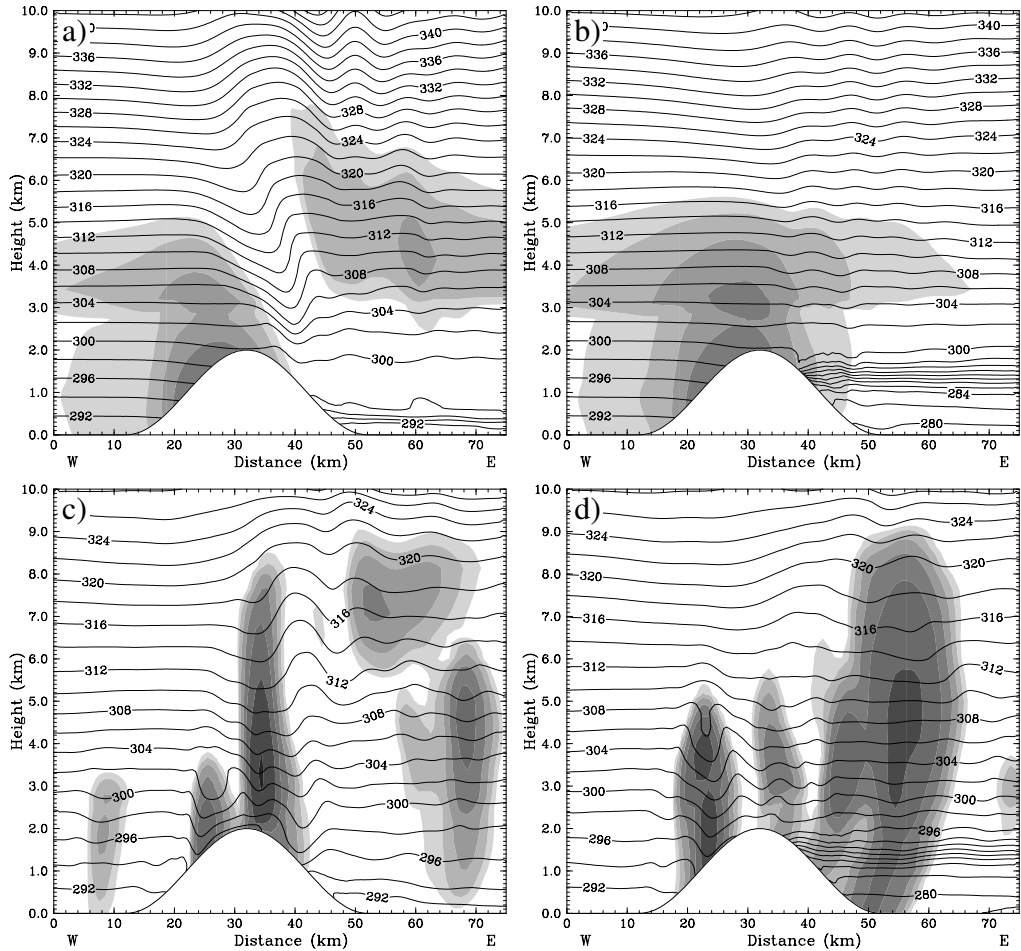
Figure 2: Vertical cross-sections of potential temperature (solid lines, contour interval 2 K) and total precipitation mixing ratio (shaded) through the centre of the western mountain ridge at $t = 18$h. Shading starts at $0.04\,\mathrm{g\,kg^{-1}}$, and each shading step denotes an increase by a factor of 2. Results are shown in the upper (lower) panels for the simulations with neutral (unstable) temperature profile, and the simulations shown in the right panels include a lee-side cold pool.

1a). On the other hand, the absolute amount of leeside precipitation is largest in the convective case. This discrepancy is related to the fact that convective cells produce more intense precipitation than stratiform clouds formed by stable orographic lifting, so that the lee-side precipitation is nonnegligible even in the absence of a cold pool. Moreover, heavy convection disturbs the formation of orographic gravity waves, thereby reducing the subsidence over the lee slope of the mountain (Fig. 2c).

It is interesting to note that the lee-side precipitation decay in the cold-pool and plateau cases can be well approximated by a straight line in the logarithmic diagrams of Fig. 1, implying that the actual decay function is roughly exponential in the absence of subsidence effects. The decay rate, as indicated by the slope of these imaginary lines, is smaller for a convective environment than for a neutral one. This can be explained by the fact that the convective cells triggered by the mountain decay quite slowly or even undergo further growth if subsidence is absent (Fig. 2d).

3.2 Strong-wind simulations

The sensitivity experiments with stronger winds (Fig. 3) show generally higher precipitation amounts over the windward slope of the mountain and a shift of the precipitation maximum towards the mountain crest, which is related to the stronger downstream advection of the precipitation particles. In the convectively unstable case, the upstream propagating cells are suppressed by the enhanced winds, so that the secondary precipitation maximum on the upwind side of the mountain disappears (Figs. 1b and 3b). In the lee of the
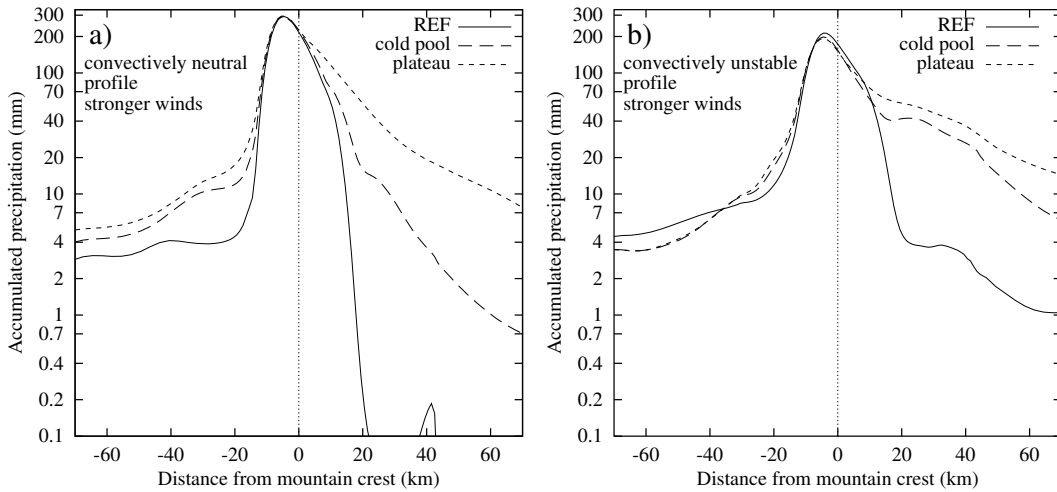
Figure 3: Same as Fig. 1, but for strong-wind simulations.

mountain, the difference between the cold-pool and the reference cases further increases. On the one hand, the intensified winds tend to reduce the leeside precipitation in the reference cases due to stronger subsidence over the lee slope (see Zängl 2005). On the other hand, the downstream advection of the precipitation increases with the wind speed, leading to more precipitation on the lee side if the subsidence is suppressed. It is also worth mentioning that the difference between the cold-pool and the plateau cases, representing an infinitely stable cold pool, is larger than for the weak-wind environment. This is related to the fact that the cold pool is no longer able to fully suppress lee-side subsidence because it is slowly eroded by the strong overlying winds. As before, the lee-side decay of the precipitation is close to exponential in the cold-pool and plateau cases.

4. CONCLUSIONS

The model results presented in this study show that the presence of a cold-air pool on the lee side of a mountain can lead to a fundamental increase in the spillover of orographic precipitation. The fractional increase typically ranges between one order of magnitude in convectively unstable cases and two orders of magnitude in nonconvective cases. However, the largest absolute amounts of leeside precipitation are found in the convective cases because convective cells decay more slowly than stratiform clouds. The impact of a leeside cold pool on the precipitation tends to increase with the ambient wind speed. In the presence of a cold pool, the precipitation decay in the lee of a mountain tends to be roughly exponential.

REFERENCES

Grell, G. A., J. Dudhia, and D. R. Stauffer, 1995: A description of the fifth-generation Penn State/NCAR mesoscale model (MM5). NCAR Tech. Note NCAR/TN-398+STR, 122 pp.

Zängl, G., 2005: The impact of lee-side stratification on the spatial distribution of orographic precipitation. *Quart. J. Roy. Met. Soc.,* in press.